Astron. Astrophys. 315, 618–624 (1996)

ASTRONOMY
AND
ASTROPHYSICS

The action of the Galactic disk on the Oort cloud comets

Qualitative study

S. Breiter[1], P. A. Dybczyński[1], and A. Elipe[2]

[1] Astronomical Observatory of the Adam Mickiewicz University, Słoneczna 36, PL 60-286 Poznań, Poland
[2] Grupo de Mecánica Espacial, Universidad de Zaragoza, E-50009 Zaragoza, Spain

Received 1 December 1995 / Accepted 17 March 1996

Abstract. Averaged equations of motion for the action of the Galactic disk on the comets from the Oort cloud are studied from the qualitative point of view. The motion is described on a sphere which reflects the actual topology of the problem. The presence and location of the equilibria is established for all cases including the class of polar orbits. A geometrical construction is proposed to analyze directly the evolution of the Laplace vector. Specifying the qualitative properties of different classes of cometary orbits may help to identify the effect of Galactic disk tides in the observed population of comets.

Key words: celestial mechanics – comets: general

1. Introduction

Tidal action by the Galactic disk on the Oort cloud is now recognized as one of the main agents susceptible of producing observable comets. The study of galactic tides usually concentrates on statistical distributions of orbital elements for comets.

We offer a geometric model in which to structure the analysis of these distributions. Our model has the advantage of incorporating the boundary cases of polar and circular orbits. The modelling transfers to cometary dynamics techniques developed in celestial mechanics for artificial satellites problems (Coffey et al. 1986) or the motion in the generalized van der Waals potential (Elipe & Ferrer 1994).

The general properties of different classes of orbits that we identify in this paper may serve as a clue in the search for the fingerprint of Galactic disk tides in the observed population of comets. The results of the paper can also be of practical value; they can be used, for example, to construct a preselection tool in Monte Carlo simulations.

Most of the algebraic operations for this paper were performed with "Mathematica" (Wolfram 1988), which also served to draw the figures.

Send offprint requests to: S. Breiter

2. The Hamiltonian of the problem

The heliocentric motion of a comet is determined by the Hamiltonian function $\mathcal{H} = \mathcal{H}_0 + \varepsilon \mathcal{H}_1$, where the Keplerian part is $\mathcal{H}_0 = -\mu/(2a)$, with the Sun's gravity parameter μ and the semi-major axis a. The unit of mass is the solar mass. The second part $\mathcal{H}_1$ has a simple oscillator form $\mathcal{H}_1 = z^2/2$ in the heliocentric Cartesian reference frame whose Oxy plane is parallell to the Galactic disk. The parameter $\varepsilon = 4\,\pi\,\mu\,\rho$ depends on the mean density of the Galactic disk ρ; adopting the value of ρ given by Bahcall (1984), one obtains $\varepsilon \approx 0.016$ Myr^{-2}. At large distances the part $\varepsilon\mathcal{H}_1$ may dominate over the Keplerian potential $U_0 = -\mu/r$, but following the generally accepted estimates of the distribution of semi-axes in the Oort cloud (see for example Duncan et al. (1987)), we can assume that most of the comets have $a < 40000$ A.U. (those with a bigger a are rather treated as interstellar comets). At this value of a one has $\varepsilon\mathcal{H}_1/\mid U_0 \mid \leq 0.1$ which allows to treat the motion as a disturbed two-body problem.

The symmetry of the potential

$$U = -\frac{\mu}{r} + \varepsilon\,\frac{z^2}{2} \tag{1}$$

with respect to the rotations around the Oz axis guarantees the conservation of the z-component H of the angular momentum. Hence, there are two integrals present in the problem: the energy integral $\mathcal{H}$ =const., and H =const. Throughout the paper we adopt the following symbols: $L = \sqrt{\mu a}$, $G = L\sqrt{1-e^2}$, and $H = Gc$ for the Delaunay momenta, l, g, h for mean anomaly, argument of perihelion, and longitude of the ascending node respectively, and c, s for the cosine and the sine of inclination.

Following Heisler and Tremaine (1986) we can replace the original Hamiltonian $\mathcal{H}$ by its average with respect to the undisturbed mean anomaly

$$\mathcal{K} = \mathcal{K}_0 + \varepsilon\,\mathcal{K}_1, \tag{2}$$

$$\mathcal{K}_0 = -\mu/(2a), \tag{3}$$

$$\mathcal{K}_1 = \tfrac{1}{4}\,a^2\,s^2\left(1 - e^2 + 5\,e^2\sin^2 g\right), \tag{4}$$

thus neglecting the periodic perturbations of order $O(\varepsilon)$. The averaged system possess three integrals of which H =const. is satisfied exactly and the remaining two $\mathcal{K}$ =const., $\mathcal{K}_0$=const. are satisfied only within the error of approximation. The latter two integrals imply a =const., L =const. , and $\mathcal{K}_1$=const. In terms of the Delaunay variables the averaged motion is reduced to the one degree of freedom problem

$$\dot{g} = \varepsilon \frac{\partial \mathcal{K}_1}{\partial G}, \qquad \dot{G} = -\varepsilon \frac{\partial \mathcal{K}_1}{\partial g}. \tag{5}$$

The equations of motion for the remaining two variables l, h involve only g, G and the two constant parameters L, H. Matese & Whitman (1989) solved the system (5) in terms of Jacobi elliptic functions. The qualitative behaviour of the solutions of (5) was studied by Heisler & Tremaine (1986) and by Matese & Whitman (1989). But both papers consider the solution curves in a (g, G) Mercator-like chart i.e. on a cylinder where the argument of perihelion g plays the role of a longitude. For obviuos geometrical reasons the solutions with $G = L$ (i.e. $e = 0$) or with $G = H$ (i.e. $s = 0$) – where g becomes undetermined – are excluded from the Mercator chart. We remedy this exclusion in the next section.

3. The motion in the general case

The proper topology of the problem is not that of a cylindric surface but this of the two-dimensional sphere $\mathcal{S}^2$. Indeed, following the approach of Coffey et al. (1986) we adopt the CDM (Coffey-Deprit-Miller) variables ξ

$$\begin{aligned} \xi_1 &= L\,G\,e\,s\cos g, \\ \xi_2 &= L\,G\,e\,s\sin g, \\ \xi_3 &= G^2 - \tfrac{1}{2}\left(L^2 + H^2\right), \end{aligned} \tag{6}$$

and find that these variables define the phase space as the sphere $\mathcal{S}^2$ with the radius

$$R_\xi = \left(\xi_1^2 + \xi_2^2 + \xi_3^2\right)^{1/2} = \tfrac{1}{2}\left(L^2 - H^2\right). \tag{7}$$

The argument of perihelion g plays the role of a longitude on the sphere (counted from the $O\xi_1$ axis counterclockwise); it is undetermined at both poles, where $\xi_1 = \xi_2 = 0$. The north pole on the sphere is the point where $\xi_3 = R_\xi$ and this implies

$$2G^2 - \left(L^2 + H^2\right) = \left(L^2 - H^2\right); \tag{8}$$

hence $G^2 = L^2$ which means $e = 0$. At the south pole, $\xi_3 = -R_\xi$ i.e $G^2 = H^2$ and this means $s = 0$. Thus, the north pole as a point represents a class of circular orbits, and the south pole is a point representing the orbits in the Galactic plane. Both points are well defined in the CDM variables as $(0, 0, \pm R_\xi)$, whereas in the Mercator map they are excluded.

The value of R_ξ, depending on the constant parameters L and H, sets the natural bounds on the eccentricity e and on the inclination i. At the south pole, where $c = 1$, the value of e reaches its maximum value $e^* = \sqrt{1 - H^2/L^2}$. Looking northward along a meridian we meet the points with smaller and smaller e, while the inclination grows because of $H/L = c\sqrt{1-e^2} =$ const. At the north pole the inclination reaches the maximum value with $c^* = H/L$ and $s^* = \sqrt{1 - H^2/L^2} = e^*$. Generally, we can treat the parallels on the sphere as the lines of constant e or equivalently as the lines of constant i. When $H^2 = L^2$ the sphere collapses into a point which represents the circular orbits in the Galactic plane. At the other extreme, $H = 0$ contains both the polar orbits ($c = 0$) and the degenerate rectilinear orbits with $G = 0$. We keep this case aside until the next section.

To obtain the equations of motion in the CDM variables we recall that, for any function u

$$\frac{du}{dt} = \{u; \mathcal{K}\}. \tag{9}$$

[N.B. $\{u; w\}$ denotes the Poisson bracket of any two functions u and w]. The easiest way to find $\dot{\xi}$ in our problem is to rewrite the Hamiltonian (4) as

$$\mathcal{K}_1 = \frac{a^2}{4\,L^2}\left(s^2\,G^2 + 5\,\xi_2^2\,G^{-2}\right), \tag{10}$$

and then to use the Poisson brackets for $\{\xi_i; \xi_j\}$ and $\{\xi_i; G\}$ given by Coffey et al. (1986) together with
$\{\xi_1; s^2\} = -2c^2\xi_2/G, \quad \{\xi_2; s^2\} = 2c^2\xi_1/G, \quad \{\xi_3; s^2\} = 0.$
For the ξ_1 we have, for example,

$$\begin{aligned} \dot{\xi}_1 = \{\xi_1; \mathcal{K}\} &= \varepsilon\,\frac{\partial \mathcal{K}_1}{\partial \xi_2}\,\{\xi_1; \xi_2\} + \\ &+ \varepsilon\,\frac{\partial \mathcal{K}_1}{\partial G}\,\{\xi_1; G\} + \varepsilon\,\frac{\partial \mathcal{K}_1}{\partial (s^2)}\,\{\xi_1; s^2\} \end{aligned} \tag{11}$$

and similarly for the remaining two variables. In this manner we obtain the equations of motion

$$\begin{aligned} \dot{\xi}_1 &= \tfrac{1}{2}\,\varepsilon\,a^2\,L^{-2} M_1\,\xi_2, \\ \dot{\xi}_2 &= \tfrac{1}{2}\,\varepsilon\,a^2\,L^{-2} M_2\,\xi_1, \\ \dot{\xi}_3 &= -5\,\varepsilon\,a^2\,G^{-1} L^{-2}\,\xi_1\,\xi_2; \end{aligned} \tag{12}$$

the coefficients M_1 and M_2 are the functions

$$M_1 = -G + 5\,\frac{\xi_2^2}{G^3} + 10\,\frac{\xi_3}{G}, \quad M_2 = G - 5\,\frac{\xi_2^2}{G^3}. \tag{13}$$

The crucial element in determining the portrait of the phase flow is the location of equilibria for system (12) and their stability.

3.1. Equilibria

The equilibria are the points on the sphere, where all the right-hand sides of the system (12) vanish at the same time. The first two points are quite easy to identify – they come from setting $\xi_1 = \xi_2 = 0$ and the critical points P_1 and P_2 are the poles of the sphere. The north pole $P_1 = \left(0, 0, (L^2 - H^2)/2\right)$ represents the circular orbits with the inclinations depending on

H, L (hence on the radius of the sphere), and the south pole $P_2 = \left(0, 0, (H^2 - L^2)/2\right)$ represents the orbits in the Galactic plane with the eccentricities depending on R_ξ. These two points are equilibria for all values of the parameters L, H allowed. Two more critical points can be found by setting $\xi_1 = 0$ and solving $M_1(\xi_2, \xi_3, G) = 0$, where $\xi_2 = L\,G\,e\,s$ and $\xi_3 = G^2 - \frac{1}{2}\left(L^2 + H^2\right)$. These two points are $P_3 = (0, \tilde{\xi}_2, \tilde{\xi}_3)$ and $P_4 = (0, -\tilde{\xi}_2, \tilde{\xi}_3)$, where

$$\tilde{\xi}_2 = \left((\sqrt{5}/2)\,H\,L\,(H^2 + L^2) - (9/4)\,H^2\,L^2\right)^{1/2}, \quad (14)$$

$$\tilde{\xi}_3 = (-L^2 - H^2 + \sqrt{5}\,H\,L\,)/2. \quad (15)$$

Because the expression under the square root should be strictly positive, P_3 and P_4 exist only when $H^2/L^2 < 4/5$. These two equilibria and the condition for their existence were found by Heisler & Tremaine (1986). Expressing $\tilde{\xi}_2$, $\tilde{\xi}_3$ in terms of Keplerian elements one can identify P_3 and P_4 as the orbits with

$$c^2 = \tfrac{4}{5}\left(1 - e^2\right), \quad (16)$$

and with the arguments of perihelia equal $\pi/2$ and $3\pi/2$ respectively.

3.2. Stability of equilibria

To determine the stability of the four points of equilibrium P_k, we form the variational equations for the system (12), replacing its right-hand sides by their linear approximations in the vicinity of a given critical point. Substituting $\xi = \xi^{(k)} + \delta\xi$, where $\xi^{(k)}$ stands for the value of ξ at the point P_k, we obtain the variational equations

$$\begin{aligned} \delta\dot{\xi}_1 &= \tfrac{1}{2}\,\varepsilon\,a^2\,L^{-2}\left[M_1^{(k)}\,\delta\xi_2 + \xi_2^{(k)}\,\delta M_1\right], \\ \delta\dot{\xi}_2 &= \tfrac{1}{2}\,\varepsilon\,a^2\,L^{-2}\left[M_2^{(k)}\,\delta\xi_1 + \xi_1^{(k)}\,\delta M_2\right], \\ \delta\dot{\xi}_3 &= \frac{-5\,\varepsilon\,a^2}{G^{(k)}L^2}\left[\xi_1^{(k)}\delta\xi_2 + \xi_2^{(k)}\delta\xi_1 - \left(\xi_1^{(k)}\xi_2^{(k)}/G^{(k)}\right)\delta G\right]. \end{aligned} \quad (17)$$

For the critical points P_1, P_2 at the poles of the sphere the variational equations become

$$\begin{aligned} \delta\dot{\xi}_1 &= \frac{\varepsilon\,a^2}{2\,L^2}\,M_1^{(1,2)}\,\delta\xi_2, \\ \delta\dot{\xi}_2 &= \frac{\varepsilon\,a^2}{2\,L^2}\,M_2^{(1,2)}\,\delta\xi_1, \\ \delta\dot{\xi}_3 &= 0. \end{aligned} \quad (18)$$

The characteristic equation for this linear differential system is

$$\lambda^2 - \tfrac{1}{4}\,\varepsilon^2\,a^4\,L^{-4}\,M_1^{(1,2)}\,M_2^{(1,2)} = 0. \quad (19)$$

At the north pole we have

$$G^{(1)} = L\,, \quad M_1^{(1)} = L\left(4 - 5\,H^2/L^2\right)\,, \quad M_2^{(1)} = L. \quad (20)$$

Accordingly, when $H^2/L^2 > 4/5$, the product $M_1^{(1)}M_2^{(1)}$ is negative and the roots of (19) are pure imaginary numbers. This means that the circular orbits are stable if and only if $5H^2 > 4L^2$. When $H^2/L^2 < 4/5$ the roots of (19) are real and the circular orbits are unstable.

As for the south pole, we have

$$G^{(2)} = H, \quad M_1^{(2)} = 4\,H - 5\,L^2/H, \quad M_2^{(1)} = H, \quad (21)$$

and the product of $M_1^{(2)}M_2^{(2)}$ is always negative. Hence, the orbits in the Galactic plane are stable for all $0 < H^2 \leq L^2$.

Because of the expressions (14) and (15), the stability analysis for P_3 and P_4 would be too complicated if it was based on the variational equations. But we already know the stability of P_1 and P_2; then we can use the *index theorem* to derive the stability of the remaining two equilibria. According to the theorem (see, e.g., (Firby & Gardiner 1991)) the sum of the indices of the fixed points is equal to the Euler characteristic of the phase space. In the present case we have stable elliptic points with the stability index +1, and unstable hyperbolic points with the index −1. The phase space being the sphere $\mathscr{S}^2$, the Euler characteristic is +2. The critical points P_3, P_4 exist when $H^2/L^2 < 4/5$. For these values of the parameters P_1 is unstable hence of index −1; P_2, however, is stable, hence of index +1. Thus the sum of the indices of P_3 and P_4 must be equal to 2; hence, for each of them the index is 1, which means that both are stable.

3.3. The motion on non polar orbits

The global dynamics of the averaged problem is illustrated in Fig. 1 where the ξ-spheres are shown as seen from the poles. The principal parameter is the ratio $\alpha = H^2/L^2$.

When α is $< 4/5$ we distinguish there three separate regions of motion:

1. The curves encircling the south pole represent the orbits for which the argument of perihelion g circulates. They reach the maximum eccentricity (i.e. minimum inclination) at $\xi_1 = 0$, i.e., at $g = \pi/2$ and $g = 3\pi/2$. The minimum of e (the most northern point) occurs at $\xi_2 = 0$, i.e., at $g = 0$ and $g = \pi$. Following the convention of Prętka & Dybczyński (1994) we call this family the solutions of "class A".
2. The curves around the stable point P_3 are the orbits with librating argument of perihelion. Their eccentricity reaches maximum and minimum values at $g = \pi/2$. We call this family the solutions of "class B_1".
3. In the neighbourhood of P_4 we find a copy of the B_1 family with g librating around $3\pi/2$ and with the extrema of e on the meridian $g = 3\pi/2$. We call this family the orbits in "class B_2".

The families A, B_1, and B_2 are separated by the two homoclinic orbits: (i) C_1 encircling the B_1 orbits, and (ii) C_2 encircling the B_2. The eccentricity of a comet on the orbit whose G and g fall at C_1 or C_2 will approach zero asymptotically with g converging to some specific value depending on α.

When the parameter α is $\geq 4/5$, the families B_1 and B_2 together with the separatrices C_1 and C_2 disappear. All the orbits – save for the poles, where g is meaningless – belong to class A with circulating g. As α tends to 1, the curves resemble more

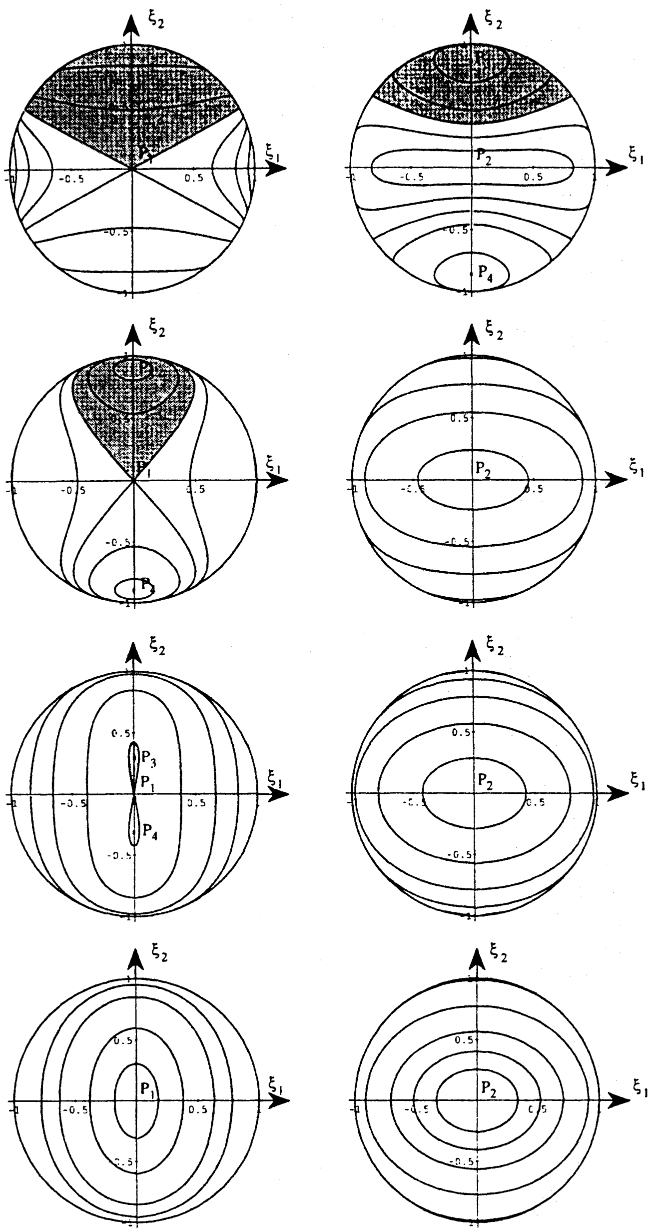

Fig. 1. Solutions in the general case traced on ξ-spheres for various values of $\alpha = H^2/L^2$. From top to bottom, $\alpha = 0.09,\ 0.64,\ 0.79,\ 0.865$. Northern hemispheres are shown at the left, and southern ones at the right. The regions of the class B_1 orbits are shaded.

and more the parallels of latitude along which eccentricity and inclination are constant.

4. Polar orbits

For polar orbits with $H = 0$ the CDM variables are insufficient. Let us set $s = 1$ in the Hamiltonian (4). Omitting the constant term $a^2/4$ we obtain the perturbation function for the polar problem

$$\widehat{\mathcal{H}}_1 = \tfrac{1}{4}\, a^2\, e^2\, (4\, \sin^2 g - \cos^2 g). \tag{22}$$

Once more we treat the problem on a sphere $\mathcal{S}^2$, but this time we use the variables introduced by Deprit (1983)

$$\zeta_1 = \sqrt{L^2 - G^2}\cos g,\ \ \zeta_2 = \sqrt{L^2 - G^2}\sin g,\ \ \zeta_3 = G.$$

The radius of the sphere defined by these variables is

$$R_\zeta = \left(\zeta_1^2 + \zeta_2^2 + \zeta_3^2\right)^{1/2} = \mid L \mid\ .$$

As in the case of the ξ-sphere, the meridians are the lines g =const. The parallels of latitude are the lines of a constant eccentricity; yet, in contrast to what we found on ξ-spheres, the equator $\zeta_3 = 0$ is the place for rectilinear orbits ($G = 0$), and not only the north pole but also the southern one represents circular orbits. The northern hemisphere consists of the prograde orbits with the angular momentum $G > 0$, and the southern hemisphere points correspond with the retrograde orbits of $G < 0$. Note, that this approach is different from the usual habit of distinguishing the prograde and retrograde orbits by the sign of H, which is no longer possible when $H = 0$.

The Hamiltonian $\widehat{\mathcal{H}}_1$ is readily expressed in terms of ζ as

$$\widehat{\mathcal{H}}_1 = \tfrac{1}{4}\, a^2\, L^{-2}\, \left(4\, \zeta_2^2 - \zeta_1^2\right)\ . \tag{23}$$

The Poisson brackets

$$\{\zeta_1;\zeta_2\} = \zeta_3,\ \ \{\zeta_2;\zeta_3\} = \zeta_1,\ \ \{\zeta_3;\zeta_1\} = \zeta_2,$$

are simple, and so is the derivation of the equations of motion

$$\begin{aligned} \dot\zeta_1 &= \{\zeta_1;\varepsilon\widehat{\mathcal{H}}_1\} = 2\,\varepsilon\, a^2\, L^{-2}\, \zeta_2\,\zeta_3, \\ \dot\zeta_2 &= \{\zeta_2;\varepsilon\widehat{\mathcal{H}}_1\} = \tfrac{1}{2}\,\varepsilon\, a^2\, L^{-2}\, \zeta_1\,\zeta_3, \\ \dot\zeta_3 &= \{\zeta_3;\varepsilon\widehat{\mathcal{H}}_1\} = -\tfrac{5}{2}\,\varepsilon\, a^2\, L^{-2}\, \zeta_1\,\zeta_2. \end{aligned} \tag{24}$$

The system admits six equilibria; these are the points
$\widehat{P}_1 = (L, 0, 0)$, $\widehat{P}_2 = (0, L, 0)$, $\widehat{P}_3 = (0, 0, L)$,
$\widehat{P}_4 = (-L, 0, 0)$, $\widehat{P}_5 = (0, -L, 0)$, $\widehat{P}_6 = (0, 0, -L)$.
Analysis of their stability is trivial, so we present only the results. The points $\widehat{P}_1$ and $\widehat{P}_4$ are the rectilinear orbits with $g = 0$ and $g = \pi$ respectively, both lying in the Galactic plane. These two equilibria are stable. The points $\widehat{P}_2$ and $\widehat{P}_5$ are the rectilinear orbits perpendicular to the Galactic plane; they have $g = \pi/2$ and $g = 3\pi/2$. They are also stable equilibria. The two unstable points $\widehat{P}_3$ and $\widehat{P}_6$ are the prograde and retrograde circular orbits.

Fig. 2 presents the motion on the ζ-sphere. We see four families of periodic solutions separated by the four homoclinic orbits connecting the poles. The separatrices are the meridians defined by $\cos g = \pm\sqrt{4/5}$. It is worth noting in Fig. 2 that all periodic solutions pass through both hemispheres and this means that any elliptic orbit perpendicular to the Galactic plane becomes rectilinear for a moment. Then a comet changes the sense of its orbital motion until its next passage through rectilinear stage. The eccentricity reaches a minimum value when g is 0, $\pi/2$, π or $3\pi/2$.

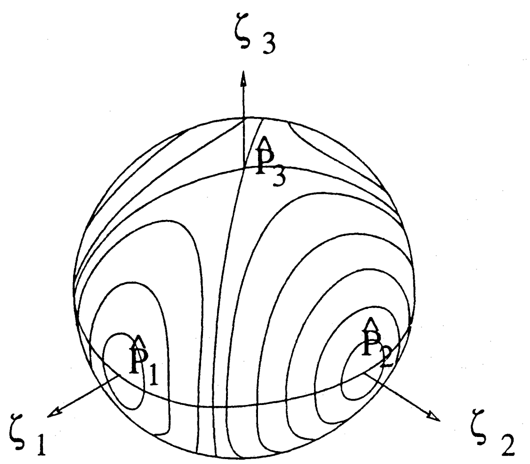

Fig. 2. Solution curves for polar orbits traced on the ζ-sphere.

5. Evolution of the Laplace vector

In cometary studes, since Byl (1983), special attention is paid to the Galactic latitude b of the perihelion. In the solution of Matese & Whitman (1989), b remains always in a zone bounded by the critical value b_c, where

$$\cos b_c = \sqrt{4/5}. \tag{25}$$

The critical value b_c is a stationary solution for b. Because of $\sin b = s \sin g$, this means that s grows at the same rate as $\sin g$ dimnishes or vice versa.

Instead of focusing on b alone, we propose a geometrical construction which shows the evolution of a heliocentric Laplace vector $\mathbf{e}$ in Galactic reference frame and explains the facts quoted above. The Laplace vector $\mathbf{e}$ is directed towards the perihelion, and its length is the eccentricity of the orbit. The Cartesian components of $\mathbf{e}$ are thus given by

$$\begin{aligned} e_1 &= e\,(\cos g \cos h - c \sin g \sin h), \\ e_2 &= e\,(\cos g \sin h + c \sin g \cos h), \\ e_3 &= e\, s \sin g. \end{aligned} \tag{26}$$

Accordingly, the latitude b of the perihelion is such that $\sin b = e_3/e$.

Taking our cue from Solov'ev (1981) we express Eq. (4) in terms of the components of $\mathbf{e}$, thereby obtaining that

$$e_1^2 + e_2^2 - 4\, e_3^2 = \beta. \tag{27}$$

The parameter β is

$$\beta = 1 - H^2/L^2 - 4\mathcal{H}_1/a^2. \tag{28}$$

Eq. (27) defines a family of quartics on which the extremity of $\mathbf{e}$ lies during the motion. All these quartics are hyperboloids with rotational symmetry around the axis Oz; they all have the same asymptotic cone.

For perturbed elliptic orbits, $-4 < \beta < 1$. Depending on the value of β, three cases occur.

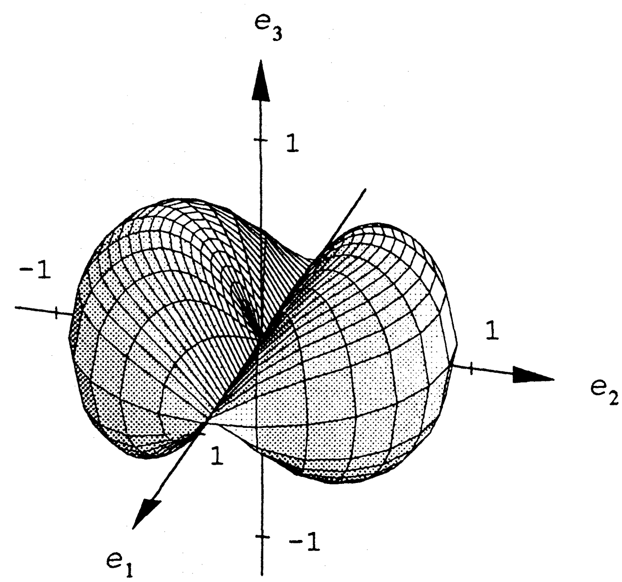

Fig. 3. The surface (31) in the nodal frame for the value of $\alpha = 0.2$.

1. For $\beta > 0$ – a hyperboloid with one sheet. The intersection of the hyperboloid with the Oxy plane is a circle of radius $\sqrt{\beta}$. This radius sets the lower bound on the minimum value of the eccentricity allowed by the initial conditions and it is associated with $b = 0$.
2. For $\beta < 0$ – a hyperboloid with two sheets. The sheets intersect the Oz axis at the points $e_3 = \pm\sqrt{-\beta/4}$, setting lower bounds on the minimum value of the eccentricity. The values of b associated with this minimum are $\pm\pi/2$.
3. For $\beta = 0$ – an asymptotic cone, the only suface which intersects the origin $e = 0$. The cone separates two families of hyperboloids thus setting a natural barrier for b in motions with $\beta \neq 0$. The angle between the Oxy plane and the surface of the asymptotic cone is precisely the value given by Eq. (25), hence a nice geometrical interpretation of this critical value.

The trajectories of the Laplace vector's extremity lie at the intersection of a quartic β = const. and of another surface, namely the one defined by the integral H =const. In the averaged system we have

$$\alpha = H^2/L^2 = (1 - e^2)\, c = \text{const.} \tag{29}$$

In the heliocentric Galactic reference frame $Ox'y'z'$ whose Ox' axis points permanently to the ascending node of the orbit (the so called *nodal frame*), the Laplace vector has the components

$$e_1 = e \cos g, \quad e_2 = e\, c \sin g, \quad e_3 = e\, s \sin g, \tag{30}$$

and the integral (29) can be expressed as

$$e_2^2 (1 - e^2)/(e_2^2 + e_3^2) = \alpha \tag{31}$$

The surface defined by this integral (let us call it "the α surface") is symmetric with respect to the coordinate planes $Ox'y'$, $Oy'z'$ and $Ox'z'$ (see Fig. 3).

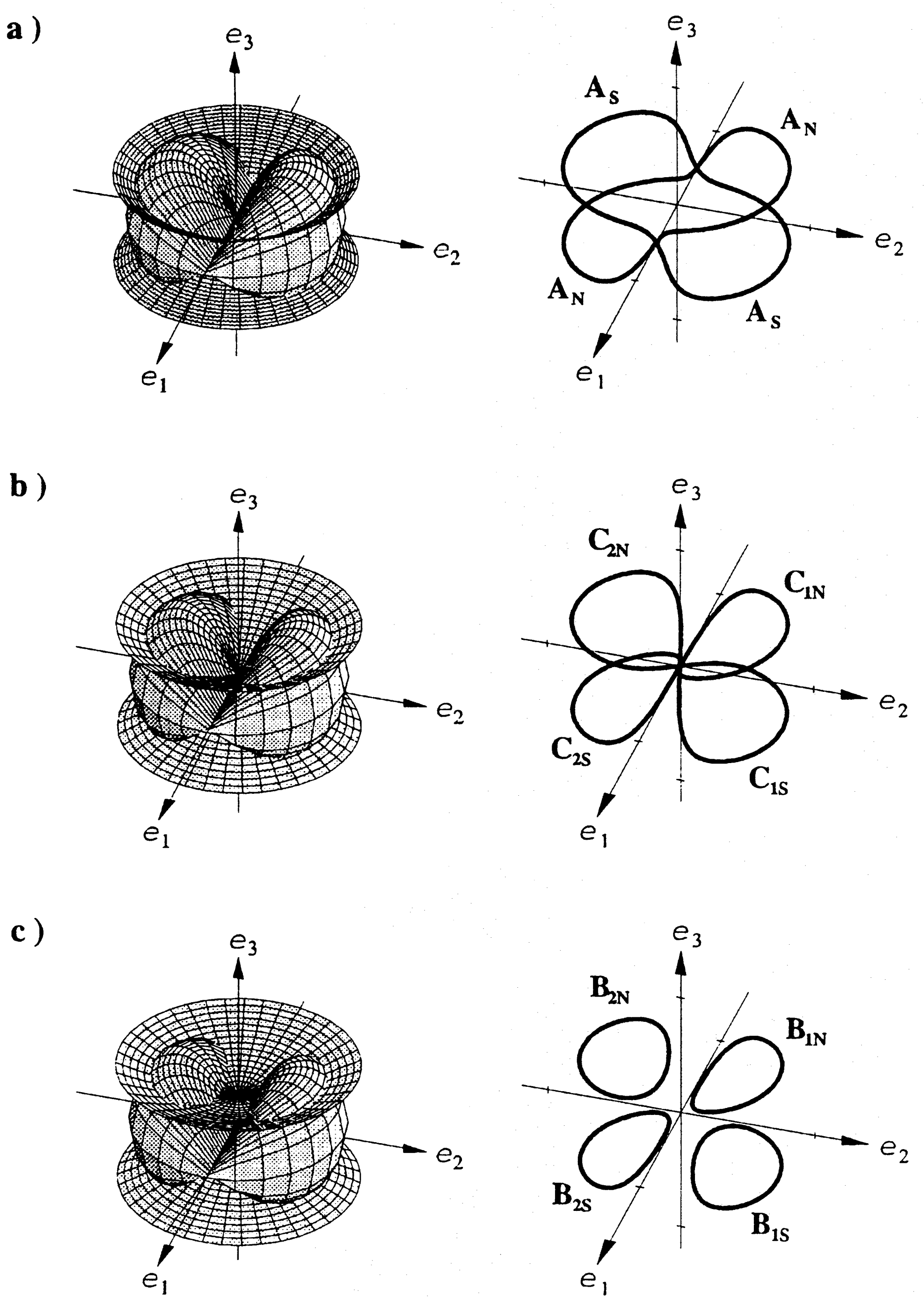

Fig. 4a–c. The intersections of $\alpha = 0.2$ surface with three β-surfaces: **a** $\beta = 0.25$, **b** $\beta = 0$, **c** $\beta = -0.25$. The intersection curves are plotted to the right and labeled according to the classification proposed in Sect. 5.

The geometrical construction based on the intersections of the surfaces (27) and (31) leads to conclusions similar to those of Sect. 2. Observe, however, that to each point on the ξ-sphere correspond two orbits of the model; they are in fact the mirror image of one another with respect to the coordinate plane $Ox'y'$. Hence to each point of $\mathscr{S}_\xi$ correspond two Laplace vectors.

1. When $\beta > 0$,
   (a) For any $0 < \alpha < 1$ the Laplace vector circulates around the axis Oz'. The latitude of perihelion oscillates around $b = 0$. The eccentricity takes the minimum value $e_{\min} = \sqrt{\beta}$ when e crosses the Galactic plane, i.e., when $b = 0$ and either $g = 0$ or $g = \pi$. We recognize here the orbits of class A. We can subdivide this family into the class A_N consisting of the orbits for which the perihelia have $e_3 > 0$ when $0 < g < \pi$ and the class A_S of orbits with $e_3 < 0$ for $0 < g < \pi$ (see Fig. 4a).
   (b) When α tends to 1 the α-surface flattens and shrinks; at the limit it collapses into a point $e = 0$. This effect coincides with the collapse of a ξ-sphere at $H = L$.
2. When $\beta < 0$.
   As it follows from solving the system of the Eqs. (27) and (31) the α-surface and β-surface intersect if and only if

$$\kappa \equiv (4 - 5\,\alpha + \beta)^2 + 20\,\alpha\,\beta \geq 0\,. \tag{32}$$

   Hence two cases arise:
   (a) When κ is > 0, the hyperboloid and the α-surface intersect along two distinct closed curves and their symmet-

ric images with respect to the Galactic plane. The two curves for $e_2 > 0$ are the class B_1 orbits, while those with $e_2 < 0$ belong to the class B_2. The eccentricity e reaches its maximum value at the minimum of $|b|$; and its minimum at the maximum of $|b|$. Both extrema occur at $g = \pi/2$ for B_1 and $g = 3\pi/2$ for B_2. In Fig. 4c the curves are further divided into into B_{1N}, B_{1S} and B_{2N}, B_{2S}, where N indicates $e_3 > 0$ and S stands for $e_3 < 0$.

(b) When $\kappa = 0$, the surfaces intersect in four points at which

$$e = \sqrt{(4 - 5\alpha - \beta)/8}. \tag{33}$$

and either $g = \pi/2$ or $g = 3\pi/2$. The latitude of the perihelion at these points is

$$\sin b = \pm\sqrt{\frac{4 - 5\alpha - 9\beta}{5(4 - 5\alpha - \beta)}}. \tag{34}$$

Looking back at the ξ-sphere we recognize here the critical points P_3 and P_4; like in the previous case and for the same reason we should distinguish P_{3N}, P_{3S}, P_{4N}, and P_{4S}.

3. The boundary case $\beta = 0$
   (a) When $0 < \alpha < 4/5$ the surfaces intersect forming the four plane curves with b having the critical value b_c mentioned in (25). These are the homoclinic trajectories C_{1N}, C_{1S}, C_{2N}, and C_{2S} which tend asymptotically to $e = 0$. They are plotted in Fig. 4b.
   (b) When $\alpha \geq 4/5$ the intersection reduces to the point $e = 0$ which is precisely the north pole P_2 of the ξ-sphere.

The geometric model for the evolution of the Laplace vector is interesting in that it leads to some information useful for example in Monte Carlo simulations.

It results from the previous discussion, that e reaches its maximum value at $e_1 = 0$ for any orbit. Under that condition we obtain from (27) and (31) that

$$e_{2(\max)} = \sqrt{(4 - 5\alpha + \beta + \sqrt{\kappa})/10}, \tag{35}$$

$$e_{3(\max)} = \sqrt{(4 - 5\alpha - 9\beta + \sqrt{\kappa})/40}. \tag{36}$$

Hence the maximum possible eccentricity

$$e_{\max} = \sqrt{(4 - 5\alpha - \beta + \sqrt{\kappa})/8}. \tag{37}$$

6. Conclusions

We have formed a geometric picture of the effect of Galactic disk tides on comets. The picture is simple and, we might say, intuitive. It sets in focus the basic features of the averaged problem: (i) that for non polar orbits there is a critical value of H/L where a pitchfork bifurcation occurs in the phase flow, and (ii) that for polar orbits a reversal in the sense of motion is possible. The analogy with the Stark effect (Deprit 1983) and the Zeeman effect (Deprit & Ferrer 1990) is striking.

Work is in progress to exploit the statistical consequences of this geometric picture for the Oort cloud cometary population.

Acknowledgements. Work presented in this paper was carried in part while Sławomir Breiter visited the University of Zaragoza; he is especially grateful for the friendly welcome and the stimulating atmosphere he found at Grupo de Mecánica Espacial. The valuable comments from André Deprit and Sebastián Ferrer are gratefully acknowledged. Criticisms by an anonymous referee proved quite valuable.

References

Bahcall J.N., 1984, ApJ, 276,169
Byl J., 1983, Moon & Planets, 29, 121
Coffey S.L., Deprit A., Miller B.R., 1986, Celest. Mech., 39, 365
Deprit A., 1983, Celest. Mech., 29, 229
Deprit A., Ferrer S., 1990, Rev. Acad. Ciencias Zaragoza, 45, 111
Duncan M., Quinn T., Tremaine S., 1987, AJ, 94, 1330
Elipe A., Ferrer S., 1994, Physical Review Letters, 72, 985
Firby P.A., Gardiner C.F., 1991, Surface Topology, Ellis Horwood Ltd, New York
Heisler J., Tremaine S., 1986, Icarus, 65, 13
Matese J.J., Whitman P.G., 1989, Icarus, 82, 389
Prętka H., Dybczyński P.A., 1994, in: Dynamics and Astrometry of Natural and Artificial Celestial Bodies, eds. K. Kurzyńska, F. Barlier, P.K. Seidelmann, I. Wytrzyszczak, Astronomical Observatory of A.M.U., Poznań, p. 299
Solov'ev E.A., 1981, JETP Lett., 34, 265
Wolfram S., 1988, Mathematica. A System for Doing Mathematics by Computer, Addison Wesley, Reading

This article was processed by the author using Springer-Verlag LaTeX A&A style file *L-AA* version 3.